Eur Radiol (2010) 20: 2482–2490
DOI 10.1007/s00330-010-1817-4

NEURO

**Peter Schramm**
**Argyro Xyda**
**Ernst Klotz**
**Volker Tronnier**
**Michael Knauth**
**Marius Hartmann**

# Dynamic CT perfusion imaging of intra-axial brain tumours: differentiation of high-grade gliomas from primary CNS lymphomas

Received: 22 January 2010
Revised: 17 March 2010
Accepted: 26 March 2010
Published online: 22 May 2010


P. Schramm (✉) · A. Xyda · M. Knauth
Department of Neuroradiology,
University of Goettingen Medical Center,
Robert-Koch-Str. 40, 37075, Goettingen, Germany
e-mail: p.schramm@med.uni-goettingen.de
Tel.: +49-551-396643
Fax: +49-551-3912868

E. Klotz
SIEMENS Healthcare Sector,
Computed Tomography,
Siemensstr. 1, 91301, Forchheim, Germany

V. Tronnier
Department of Neurosurgery,
University Schleswig-Holstein,
Campus Luebeck - Haus 12, Ratzeburger Allee 160, 23538, Luebeck, Germany

M. Hartmann
Division of Neuroradiology,
Department of Neurology,
University of Heidelberg Medical Center,
Im Neuenheimer Feld 400, 69120, Heidelberg, Germany

**Abstract**
*Introduction:* Perfusion computed tomography (PCT) allows to quantitatively assess haemodynamic characteristics of brain tissue. We investigated if different brain tumor types can be distinguished from each other using Patlak analysis of PCT data. *Methods:* PCT data from 43 patients with brain tumours were analysed with a commercial implementation of the Patlak method. Four patients had low-grade glioma (WHO II), 31 patients had glioblastoma (WHO IV) and eight patients had intracerebral lymphoma. Tumour regions of interest (ROIs) were drawn in a morphological image and automatically transferred to maps of cerebral blood flow (CBF), cerebral blood volume (CBV) and permeability ($K^{Trans}$). Mean values were calculated, group differences were tested using Wilcoxon and Mann Whitney *U*-tests. *Results:* In comparison with normal parenchyma, low-grade gliomas showed no significant difference of perfusion parameters ($p>0.05$) , whereas high-grade gliomas demonstrated significantly higher values ($p<0.0001$ for $K^{Trans}$, $p<0.0001$ for CBV and $p=0.0002$ for CBF). Lymphomas displayed significantly increased mean $K^{Trans}$ values compared with unaffected cerebral parenchyma ($p=0.0078$) but no elevation of CBV. High-grade gliomas show significant higher CBV values than lymphomas ($p=0.0078$). *Discussion:* PCT allows to reliably classify gliomas and lymphomas based on quantitative measurements of CBV and $K^{Trans}$.

**Keywords** Computed tomography · Perfusion · Brain tumours · Gliomas · Lymphomas

## Introduction

A variety of imaging techniques has been described for the assessment of cerebral perfusion. These techniques have been primarily used to assess cerebral ischaemia [1, 2]; however, the range of perfusion applications is being expanded, including the diagnostic field of cerebral tumours. Perfusion-weighted magnetic resonance imaging (PWI) has been proven to provide additional valuable information about intra-axial brain tumours [3–6]. A correlation among perfusion parameters, tumour grade and treatment response has already been demonstrated through the non-invasive measurement of regional cerebral blood volume (CBV), regional cerebral blood flow (CBF) and permeability (PMB) as a measure of blood-brain barrier disruption by PWI techniques [3–6]. Furthermore, perfusion imaging has shown promising results for distinguishing recurrence from radionecrosis, but also for differentiating cerebral tumour lesions, such as lymphomas and gliomas [3].

Non-invasive assessment of cerebral perfusion by means of dynamic perfusion computed tomography (PCT) has also been used for the evaluation of brain tumours. PCT has exhibited a number of advantages over

PWI, the most important of which is the linear relation between density changes and the tissue concentration of the contrast agent. Moreover, PWI, because of susceptibility artefacts generated by haemorrhage or various mineral depositions, can create diagnostic concerns in post-treatment tumour patients. CT is often the first imaging technique that is performed in patients suffering from neurological symptoms caused by brain tumours. Even though non-enhanced CT is not really the imaging technique of choice for a detailed neuroradiological diagnosis of brain tumours, getting additional haemodynamic information from the same device without having to shift technique appears to be attractive [7]. PCT renders important information in patients with intra-axial brain tumours, allowing differentiation not only between low-grade and high-grade gliomas but also between high-grade gliomas and lymphomas, by quantifying regional CBV, CBF and permeability of the blood-brain barrier with a single acquisition [7]. Because tumour neoangiogenesis and neovascularisation play an important role in tumour growth and spread, measurement of perfusion characteristics enables the prediction of tumour grade, the determination of treatment options and the assessment of treatment response and prognosis [8].

The aim of our study was to prospectively evaluate the feasibility and efficacy of PCT in the preoperative differential diagnosis of intra-axial brain tumours. Furthermore, we tried to explore a non-invasive way of quantifying and classifying the characteristics of cerebral gliomas and lymphomas according to their regional perfusion parameters.

## Materials and methods

Between 2004 and 2008, 49 consecutive patients with intra-axial brain tumours and tumour-like lesions were enrolled prospectively in our study. All patients included in our study had not received any kind of biopsy or treatment at the time of examination. Patients who were planned to undergo biopsy because of newly diagnosed intra-axial brain tumours received unenhanced brain CT in order to locate the lesion. The unenhanced CT was then used to plan the slice positions of PCT in order to hit the centre of the tumour. PCT was then followed by stereotactic or open biopsy in order to assess the histopathological grade of the examined tumour.

All radiological analyses were conducted in a blind fashion with regard to the patients' identity, clinical data and initial diagnostic CT findings. The data were analysed by two experienced neuroradiologists (P.S., M.H.). Raters did not receive any information about the affected hemisphere. They evaluated unenhanced CT independently so as to designate the location and the margins of the tumour and to determine the sections that contained the largest part of solid tumour. In these sections, PCT analysis was carried out. Disputes between interpreters were decided by consensus.

Written informed consent was obtained from all participating patients. The study protocol was approved by the local Ethics and Scientific Committees of Heidelberg University School of Medicine.

### CT perfusion imaging

All PCTs were obtained with a standard 50-s PCT (Siemens Somatom Volume Zoom). The parameters for the PCT were 80 kV and 250 mAs, one image, slice collimation 2 × 10 mm. For the PCT, 33 patients received a biphasic protocol consisting of a total of 60 ml of a non-ionic contrast agent (Imeron 400, Bracco Imaging, Konstanz, Germany), injected using a high-pressure injector through an 18-gauge intravenous line in the cubital vein with a start delay of 4 s. The biphasic injection protocol consisted of 30 ml contrast material at a rate of 5 ml/s, immediately followed by another 30 ml at a rate of 2 ml/s and finally 20 ml of a saline chasing bolus at a rate of 2 ml/s. From every selected axial section 50 consecutive images were acquired with a time interval of 1 s.

In 16 patients, a different contrast protocol was applied. We utilised 36 ml of a non-ionic high concentrated iodine contrast agent (Imeron 400, Bracco Imaging, Konstanz, Germany) with an injection rate of 6 ml/s.

In order to verify that the different contrast protocols did not significantly influence the perfusion parameters, they were compared for the high-grade glioma patients, as high-grade gliomas represent the largest group in our series. Furthermore, all perfusion parameters in this histopathological subgroup were found to be significantly higher than normal parenchyma. The potential heterogeneity due to different contrast material protocols was assessed through the comparison of all perfusion parameters (Table 1). No significant difference was found between the two subgroups. Therefore they were evaluated as one entity for further statistical analysis.

### Data processing and analysis

All PCT images and parameters were analysed using a standard workstation (MMWP, Siemens, Erlangen, Germany) with commercially available software (Volume Perfusion CT, Siemens, Erlangen, Germany). Automatic segmentation was applied to exclude non-parenchymal pixels such as bone, cerebrospinal fluid (CSF) or vessels. In order to obtain peak vascular enhancement in blood, the superior sagittal sinus was selected as the venous reference vessel for the PCT process, as with 10-mm-thick axial sections a reliable absolute density evaluation of cerebral arteries can be restricted because of partial volume effects [1]. By applying the perfusion software, quantitative parameter images were generated from the time-attenuation curves. For each patient, four types of parameter maps were calculated for each section: temporal maximum intensity projection (MIP) in Hounsfield units (HU), CBV (ml/100 ml), CBF (ml/100 ml/min) and the

**Table 1** Comparison of different contrast material protocols: Mann-Whitney *U*-test showed no significant difference between the two subgroups (values expressed as median and interquartile range)

| | Contrast material protocol 1 ($n$=19) | Contrast material protocol 2 ($n$=10) | $p$ |
|---|---|---|---|
| $K^{trans}$ (ml/100 ml/min) | 5.80 (4.43–9.45) | 4.04 (3.27–9.99) | >0.05 |
| CBV (ml/100 ml) | 5.37 (4.36–6.74) | 5.58 (4.71–7.55) | >0.05 |
| CBF (ml/min) | 75.69 (62.12–108.73) | 110.00 (84.99–132.18) | >0.05 |

volume transfer constant $K^{Trans}$ as a measure of permeability (ml/100 ml/min). CBF was calculated using the maximum slope model [9], CBV and $K^{Trans}$ were calculated using Patlak analysis (Appendix 1). The shape of the arterial input function necessary for the Patlak analysis was automatically determined from branches of the MCA or ACA, the peak of the input function was normalized to the peak of the superior sagittal sinus.

The raters then independently determined and manually drew regions of interest (ROIs) on the maps. Initially, ROIs were drawn on the MIP images, on the solid part of tumour, trying to exclude areas with necrosis or vessels. The ROIs were then automatically copied onto the perfusion maps and corresponding CBV, CBF and $K^{Trans}$ values were acquired. For every patient, reference ROIs were also drawn on the healthy contralateral hemisphere and perfusion parameters were obtained as control values.

### Statistical analysis

The results are presented as mean ± standard deviation (SD) and range for numerical variables and absolute numbers (percentage). Initially, the normal distribution of numerical variables through box plots, histograms and Q-Q plots was tested. The values of the parameters obtained from PCT analysis followed the Gaussian distribution except in a case of an oligodendral mixed glioma which was not included in the analysis. Wilcoxon paired sample test was used for the comparisons between tumour lesions and healthy parenchyma, because the data were used for the comparisons among the different histological subgroups. All $p$ values reported are two-tailed. Statistical significance was set at 0.05 and analyses were conducted using SPSS statistical software version 12.0 (SPSS, Chicago, Ill., USA).

## Results

Patients' demographics and clinical characteristics are presented in Table 2. The mean age of the patients at diagnosis was 58.5±11.6 years and ranged from 33 to 75 years. Four patients with cerebral metastases were excluded from the perfusion analysis as their perfusion physiology differed depending on the primary tumour characteristics. Furthermore, no comparisons between the two patients with inflammatory lesions were carried out because of the heterogeneity and the limited number of patients in this subgroup.

Data from 43 patients were finally analysed. Patients were classified into three histopathological subgroups (low-grade gliomas, high-grade gliomas, lymphomas).

### Comparison of perfusion parameters between affected and normal cerebral parenchyma

The mean values for $K^{Trans}$, CBV and CBF values for the study subgroups and the comparisons with the control healthy parenchyma are summarised in Table 3. No significant difference in the perfusion parameters was found between areas of low-grade gliomas and normal cerebral parenchyma ($p$>0.05 for all analysed perfusion parameters). High-grade gliomas, on the other hand, demonstrated significantly higher values of all perfusion parameters compared with normal cerebral parenchyma ($p$<0.0001 for $K^{Trans}$, $p$<0.0001 for CBV and $p$=0.0002 for CBF). Lymphomas displayed significantly increased mean permeability values compared with unaffected cerebral parenchyma ($p$=0.0078 for $K^{Trans}$), whereas no significant difference was noted between the mean CBV and CBF values ($p$=0.55 for CBV, $p$=0.25 for CBF).

### Comparison of perfusion parameters between different histopathological subgroups

Low-grade gliomas were excluded from the comparisons among the histopathological subgroups because their low number precluded an efficient statistical analysis. Figures 1, 2 and 3 show the comparison between high-grade gliomas

**Table 2** Patients' demographics and clinical characteristics

| | $n$ | % |
|---|---|---|
| Male | 30 | 61.2 |
| Female | 19 | 38.8 |
| High-grade gliomas | 31 | 63.3 |
| Lymphomas | 8 | 16.3 |
| Low-grade gliomas | 4 | 8.15 |
| Metastases | 4 | 8.15 |
| Infectious tumour-like lesions | 2 | 4.1 |

**Table 3** Comparison of perfusion parameters between affected and normal cerebral parenchyma. Values are expressed as mean ± SD

| Histopathological subgroup ($p$) | $K^{Trans}$ (ml/100 ml/min) | | $p^a$ | CBV (ml/100 ml) | | $p^a$ | CBF (ml/100 ml/min) | | $p^a$ |
|---|---|---|---|---|---|---|---|---|---|
| | Lesion | Control | | Lesion | Control | | Lesion | Control | |
| Low-grade gliomas (4) | 3.73±5.35 | 1.66±1.79 | 0.25 | 3.28±0.46 | 2.96±0.42 | 0.38 | 62.28±16.91 | 65.80±5.50 | 0.88 |
| High-grade gliomas (31) | 6.58±3.68 | 0.86±0.79 | <0.0001 | 6.03±2.18 | 3.22±0.42 | <0.0001 | 97.63±41.17 | 64.45±7.84 | 0.0002 |
| Lymphomas (8) | 11.96±10.66 | 1.31±1.79 | 0.0078 | 3.79±1.95 | 3.14±0.42 | 0.55 | 82.79±40.03 | 64.87±9.61 | 0.25 |

[a] $p$ compared with healthy parenchyma values (control) using Wilcoxon test

and lymphomas (Mann-Whitney $U$-test): whereas no statistical difference was found for CBF ($p$=0.3567) and $K^{Trans}$ ($p$=0.1394), high-grade gliomas showed a significant elevation of CBV in comparison to lymphomas ($p$=0.0078). However, higher mean permeability values, though not statistically significant, were observed in lymphomas in comparison with high-grade gliomas.

## Discussion

In this study, our objective was to quantify the absolute PCT parameters of intracerebral tumours. We report one of the largest series concerning the application and efficacy of PCT in the preoperative histopathological grouping of cerebral intra-axial tumours. By applying a CT perfusion method and based on the absolute perfusion parameters, we differentiated cerebral lymphomas from high-grade gliomas (Figs. 4, 5).

Dynamic perfusion imaging is based on the assessment of tissue-related distribution of the contrast medium, which acts as a tracer. Microvascularisation and diffusion across the endothelial membrane into the interstitial space determine the distribution of contrast agent after infusion. The absolute perfusion parameters correspond to the microvascular density, in histopathological examination, which has been considered to be the 'gold standard' for such an evaluation, because of its direct association with angiogenic growth factor expression, tumour growth, and metastatic occurrence [10, 11]. In accordance with previously published studies, significantly increased CBV was noted in high-grade gliomas. The increased vascular proliferation of the neoplastic tissue and the hypothesis that feeding arterioles are more vasodilated than normal in neoplasms support these findings [8, 12, 13].

Increased vascular permeability has also been correlated with malignancy and has been evolving as a surrogate marker of tumour angiogenesis and, thus, tumour grade [14]. Higher permeability has been associated with higher tumour grade and has also been shown to decrease, responding to antiangiogenic therapy [3, 15–17]. Our results demonstrated significantly higher permeability values for both high-grade gliomas and lymphomas in comparison with healthy tissue. Both entities are characterised by a histopathologically proven blood-brain barrier disturbance [18, 19].

It has already been shown that PWI provides valuable information concerning tumour perfusion, facilitating the preoperative classification and grading of gliomas [3–6]. Our data stress the role of PCT in the preoperative differential diagnosis of primary central nervous system lymphomas (PCNSL) from high-grade gliomas. PCNSL, a discrete histopathological entity, constitute up to 6% of malignant central nervous system (CNS) tumours [20].

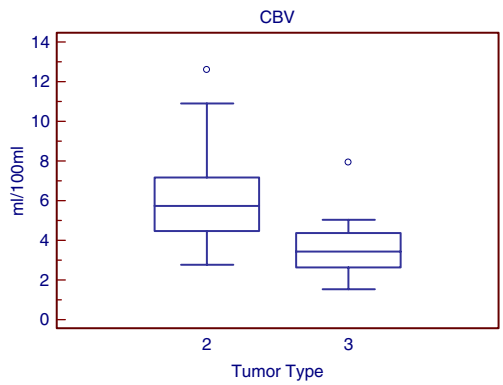


**Fig. 1** Comparison of high-grade gliomas (tumour type 2) and lymphomas (tumour type 3): Mann-Whitney $U$-test showed significant elevation of CBV within high-grade gliomas compared with lymphomas ($p$=0.0078)

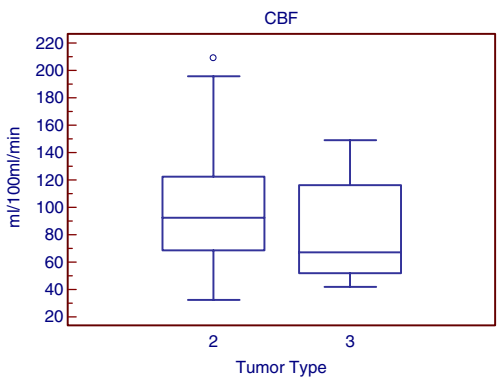


**Fig. 2** Comparison of high-grade gliomas (tumour type 2) and lymphomas (tumour type 3): Mann-Whitney $U$-test showed no significant difference in CBF within the tumour tissue ($p$=0.3567)

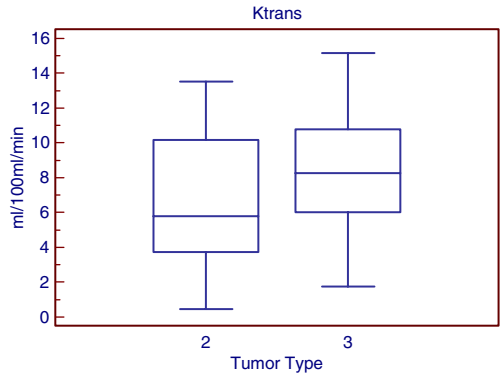


**Fig. 3** Comparison of high-grade gliomas (tumour type 2) and lymphomas (tumour type 3): Mann-Whitney *U*-test showed no significant difference in $K^{Trans}$ within the tumour tissue ($p$=0.1394)

Although PCNSL present certain characteristic magnetic resonance imaging (MRI) findings, it can be difficult or even impossible to differentiate them, on the basis of imaging features, from high-grade gliomas on standard CT or MRI, because of their diffuse infiltrative growth [21, 22]. Histopathologically, contrary to high-grade gliomas, PCNSL are characterised by the absence of neovascularisation. Our results show that lymphomas can be differentiated from high-grade gliomas by comparing CBV and CBF parameters using PCT. Both histopathological entities presented significantly higher permeability values compared with normal brain parenchyma, but only high-grade gliomas presented with significantly higher values of regional CBV and CBF parameters than those of normal cerebral parenchyma. Our results are comparable with those previously reported for a series of patients who

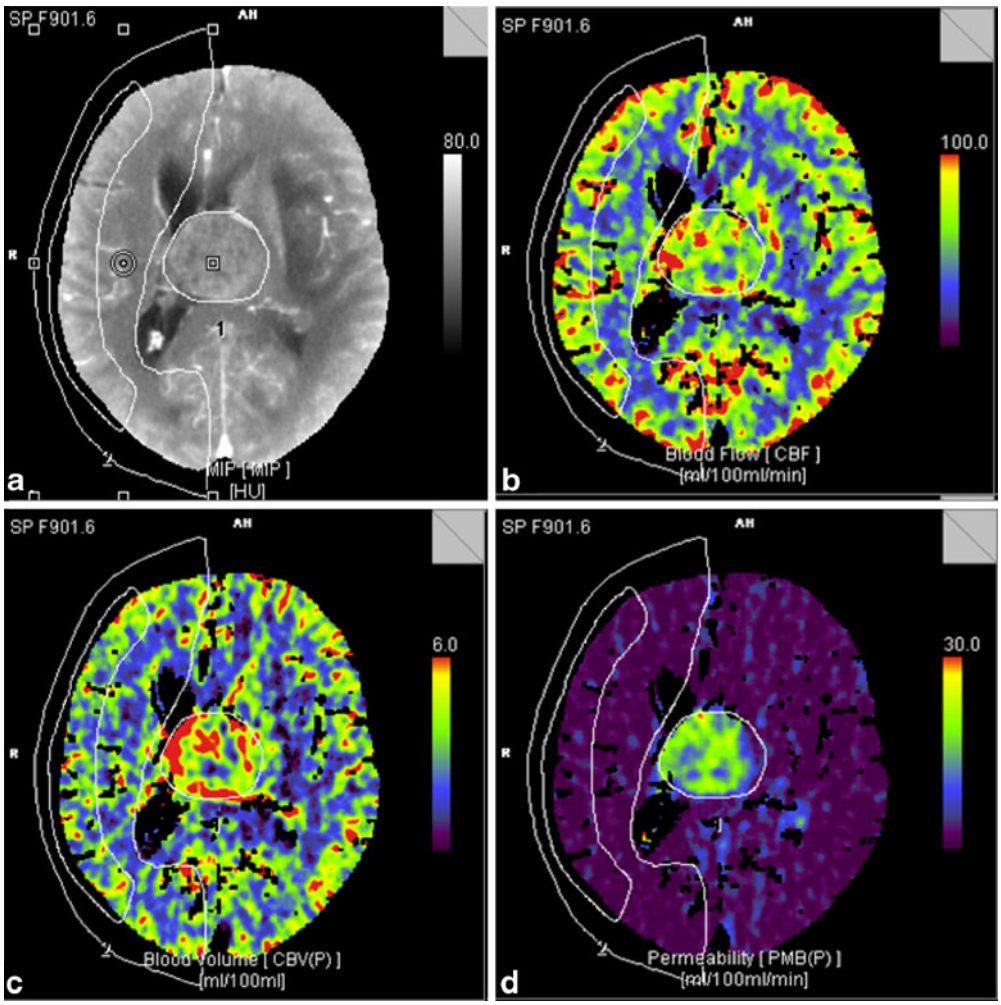


**Fig. 4** A 58-year-old man with histopathological diagnosis of glioblastoma multiforme WHO IV. Axial contrast-enhanced MIP reconstruction image (**a**) shows a contrast-enhanced mass, which demonstrates intensely elevated blood flow (**b**) and volume (**c**) as well as strongly increased regional $K^{trans}$ (**d**) in comparison with the normal cortical and subcortical cerebral parenchyma

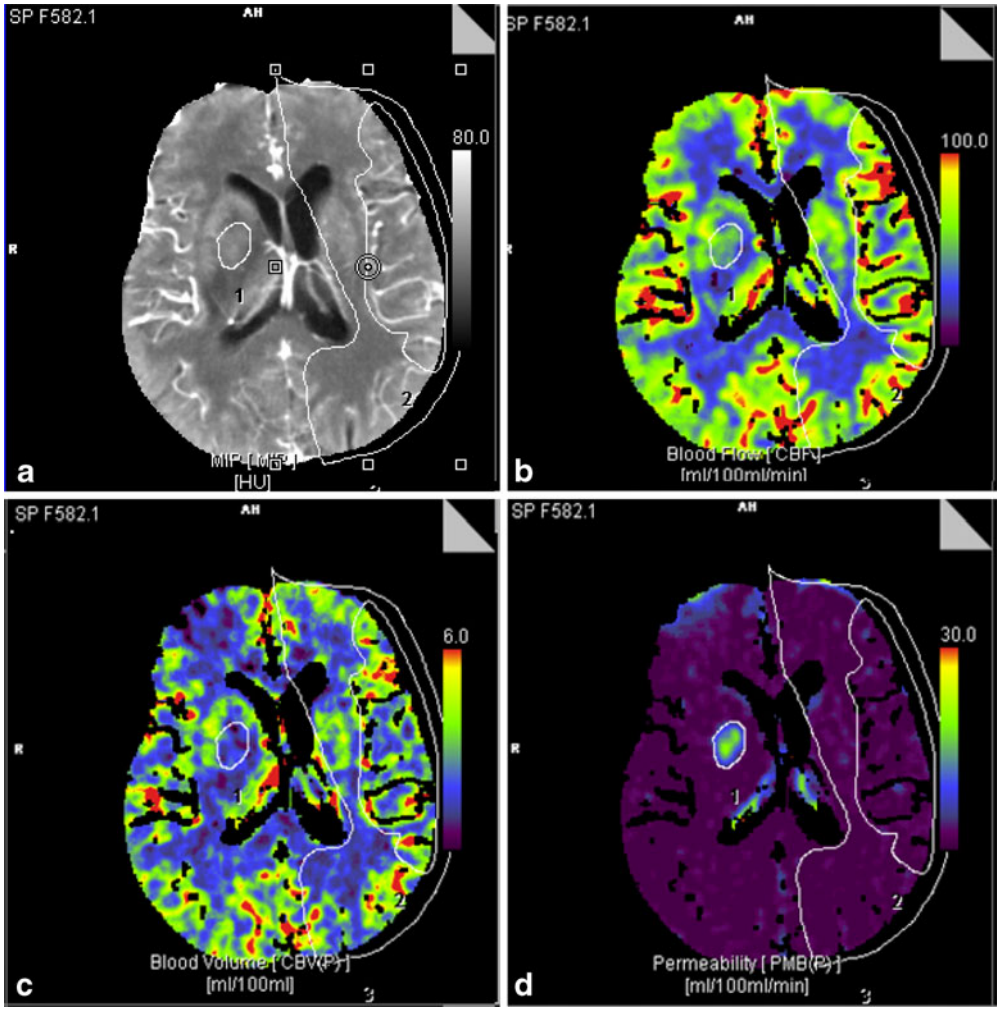


**Fig. 5** A 72-year-old woman with histopathological diagnosis of primary cerebral lymphoma. In comparison with the contralateral normal cerebral parenchyma, the lesion depicted in the right lentiform nucleus demonstrates the typical perfusion characteristics of lymphoma: enhancement (**a**), no significant increase in CBF (**b**) or CBV values (**c**), though intensely increased regional permeability ($K^{Trans}$, **d**), indicating a massive disturbance of the blood-brain barrier

underwent PWI [19]. Because PCNSL and high-grade gliomas require different therapeutical management and differ in prognosis, precise diagnosis is crucial [20, 23].

Gliomas, the most frequent cerebral tumours in adults, exhibit varying degrees of cellular and nuclear pleomorphism, mitotic activity, vascular proliferation and necrosis [24, 25]. This histopathological heterogeneity explains the difficulties concerning the preoperative assessment and biopsy and thus histopathological grading. Histopathological assessment of tissue, the current standard for tumour grading, presents inherent limitations, including sampling errors, intra-observer variation and the changing nature of central nervous system tumours [26, 27]. Accurate histopathological diagnosis is crucial to define the appropriate management and prognosis according to tumour grade. For low-grade gliomas, conservative treatment and monitoring for detecting transformation or active proliferation are of great importance. Because the degree of vascular proliferation is one of the most critical elements in the determination of tumour grade and prognosis, the preoperative non-invasive assessment and quantification of glioma vascularity can be helpful to determine the malignant potential of the tumour, to select an appropriate biopsy site, to evaluate transition from low-grade to a high-grade glioma, and also to monitor treatment response [28]. Despite the small number of patients with low-grade gliomas, our data implicate that high-grade gliomas could be differentiated from low-grade gliomas on the basis of all three PCT parameters studied. Low-grade gliomas exhibited no different perfusion parameters compared with normal parenchyma (Fig. 6).

In spite of the feasible advantages of PCT over PWI, the relative limitations of PCT and consequently of our study are the radiation dose involved with the procedure and also the limited coverage area of the cerebral parenchyma compared with PWI. The latter limitation could be overcome in the future with the new volume PCT technique, which enables the measurement of the whole brain and three-dimensional qualitative and quantitative imaging. Thus, whole-brain PCT could lead to even more precise grading of intra-axial brain

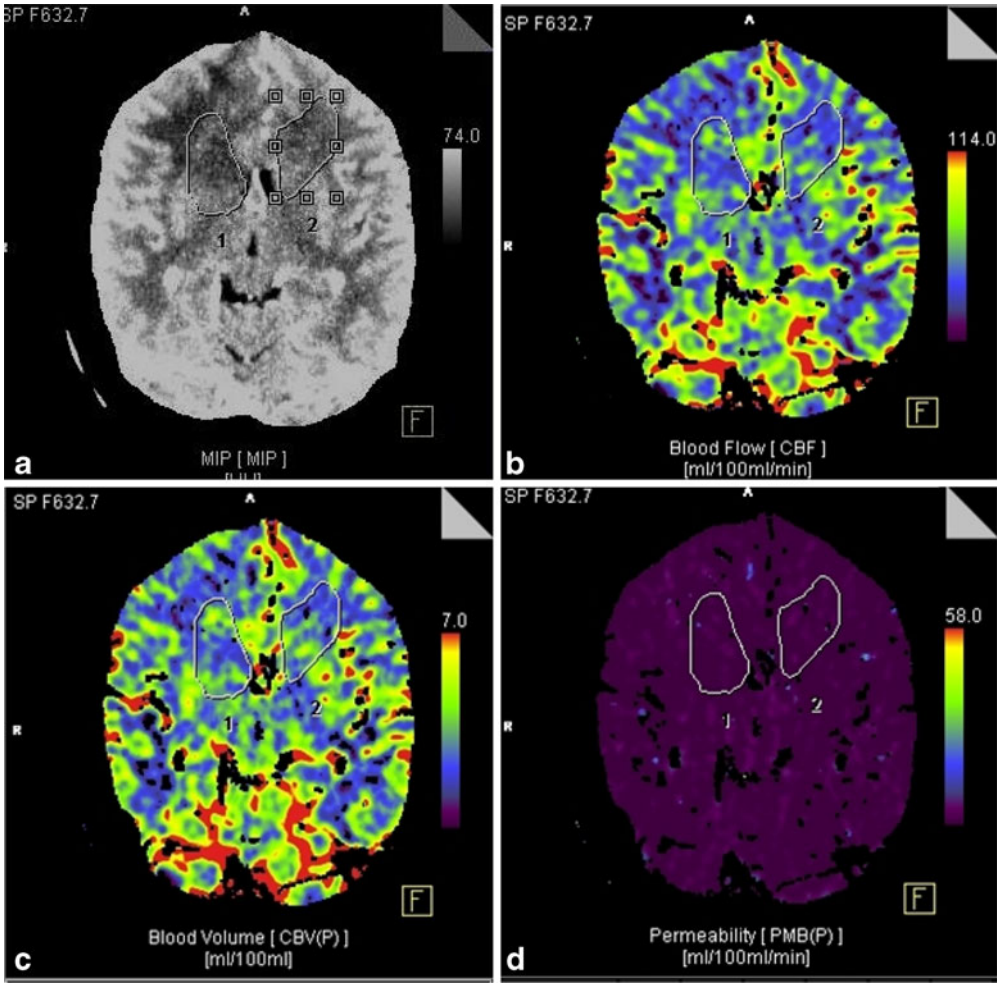


**Fig. 6** A 42-year-old man with histopathological diagnosis of low-grade glioma WHO II. The contrast-enhanced MIP image (**a**) shows no enhancement within the tumour in the right frontal lobe (*1*). The perfusion maps reveal no significant difference in the perfusion parameters CBF (**b**), CBV (**c**) and $K^{\mathrm{Trans}}$ (**d**) between the lesion (*1*) and the unaffected side (*2*)

tumours. Potential limitations also include the different contrast agent protocols applied. However, we statistically demonstrated no methodological heterogeneity regarding the perfusion parameters generated.

In conclusion, with the role of imaging beginning to shift towards providing complementary information concerning tumour dynamics and physiology, our results revealed the promising and determinant role of the perfusion technique in the preoperative histopathological assessment of cerebral intra-axial tumours. By detecting and quantifying microvascular density and capillary permeability PCT helps to distinguish cerebral lymphomas from high-grade gliomas and facilitates the preoperative histopathological grouping of brain gliomas. Information obtained by the in vivo monitoring of tumour proliferation and angiogenesis may support the role of PCT in the clinical routine not only preoperatively but also in the post-treatment assessment and follow-up of patients with intra-axial cerebral tumours. However, additional studies are required to differentiate between patients with high- and low-grade gliomas as well as between those with radionecrosis and recurrence.

## Appendix 1

Patlak analysis can be derived from a two-compartment model that describes the one-way transfer of contrast material from the intravascular space to the extravascular space, i.e. there is no significant backflow during the examination time. At any time point, the tissue concentration of contrast material is equivalent to the sum of the intravascular and extravascular concentrations of contrast material as denoted by the following equation:

$$C(t) = CBV\, C_A(t-\Delta t) + K^{trans} \int_0^{t-\Delta t} C_A(\tau) d\tau$$

where $C(t)$ is the concentration of contrast material within the tissue, $CBV$ is the cerebral blood volume, $C_{\mathrm{A}}(t)$ is the concentration of contrast material in blood (the arterial input function AIF) and $K^{\mathrm{Trans}}$ is the volume transfer constant [29]; $\Delta t$ describes the time it takes the input function to travel to the tissue voxel; $\Delta t$ is determined

automatically by cross correlation analysis of the AIF with the voxel TAC separately for every voxel.

Dividing the equation by $C_A(t)$ produces the linear relationship

$$\frac{C(t)}{C_A(t-\Delta t)} = CBV + K^{trans}\frac{\int_0^{t-\Delta t} C_A(\tau)d\tau}{C_A(t-\Delta t)}$$

By fitting a straight line to the data points, $K^{\mathrm{Trans}}$ can be derived from the slope of this line and CBV from the intercept.

$K^{\mathrm{Trans}}$ describes the portion of blood flow $F$ that is extracted into the extravascular space, i.e. $K^{\mathrm{Trans}} = E \cdot F$, with the extraction fraction $E$ (**EK1**), which is defined as

$$E = 1 - e^{-PS/F(1-Hct)}$$

$PS$ is the permeability–surface area product and $Hct$ the haematocrit value.

Note that we define $K^{\mathrm{Trans}}$ with respect to whole blood flow, while in MR perfusion imaging it is typically defined with respect to plasma flow: $K^{\mathrm{Trans}} = K^{\mathrm{Trans}}(\mathrm{MRI})/(1 - Hct)$.

From these relationships it can be derived that for tumours which are well perfused, $K^{\mathrm{Trans}}(1 - Hct)$ is approximately equal to $PS$.



## References


1. Koenig M, Kraus M, Theek C, Klotz E et al (2001) Quantitative assessment of the ischemic brain by means of perfusion-related parameters derived from perfusion CT. Stroke 32:431–437
2. Schramm P, Schellinger PD, Klotz E et al (2004) Comparison of perfusion computed tomography angiography source images with perfusion-weighted imaging and diffusion-weighted imaging in patients with acute stroke of less than 6 hours duration. Stroke 35:1652–1658
3. Roberts HC, Roberts TP, Bollen AW et al (2000) Quantitative measurement of microvascular permeability in human brain tumors achieved using dynamic contrast-enhanced MR-imaging: correlation with histologic grade. AJNR Am J Neuroradiol 21:891–899
4. Law M, Yang S, Babb JS et al (2004) Comparison of cerebral blood volume and vascular permeability from dynamic susceptibility contrast-enhanced perfusion MR imaging with glioma grade. AJNR Am J Neuroradiol 25:746–755
5. Gossmann A, Helbich TH, Kuriyama N et al (2002) Dynamic contrast-enhanced magnetic resonance imaging as surrogate marker of tumor response to angiogenic therapy in a xenograft model of glioblastoma multiform. J Magn Reson Imaging 15:233–240
6. Cao Y, Shen Z, Chenevert TL et al (2006) Estimate of vascular permeability and cerebral blood volume using Gd-DTPA contrast enhancement and dynamic T2*-weighted MRI. J Magn Reson Imaging 24:288–296
7. Schramm P (2007) High concentration contrast media in neurological multidetector-row CT-applications: implications for improved patient management in neurology and neurosurgery. Neuroradiology 49(Suppl 1):S35–S45
8. Jain J, Ellika SK, Scarpace L et al (2008) Quantitative estimation of permeability surface-area product in astroglial brain tumors using perfusion CT and correlation with histopathologic grade. AJNR Am J Neuroradiol 29:694–700
9. Klotz E, König M (1999) Perfusion measurements of the brain: using dynamic CT for the quantitative assessment of cerebral ischemia in acute stroke. Eur J Radiol 30:170–184
10. Phongkitkarun S, Kobayashi S, Kan Z et al (2004) Quantification of angiogenesis by functional computed tomography in Matrigel model in rats. Acad Radiol 11:573–582
11. Weidner N (1995) Intratumor microvessel density as a prognostic factor in cancer. Am J Pathol 147:9–19
12. Ding B, Ling HW, Chen KM et al (2006) Comparison of cerebral blood volume and permeability in preoperative grading of intracranial glioma using CT perfusion imaging. Neuroradiology 48:773–781
13. Cenic A, Nabavi DG, Craen RA et al (2000) A CT method to measure haemodynamics in brain tumors: Validation and application of cerebral blood flow maps. AJNR Am J Neuroradiol 21:462–470
14. van Dijke CF, Brasch RC, Roberts TP et al (1996) Mammary carcinoma model: correlation of macromolecular contrast-enhanced MR imaging characterization of tumor microvasculature and histologic capillary density. Radiology 198:813–818
15. Jain RK, Tong RT, Munn LL (2007) Effect of vascular normalization by antiangiogenic therapy on interstitial hypertension, peritumor edema, and lymphatic metastasis: insights from a mathematical model. Cancer Res 67:2729–2735
16. Daldrup H, Shames DM, Wendland M et al (1998) Correlation of dynamic contrast-enhanced MR imaging with histologic tumor grade: comparison of macromolecular and small-molecular contrast-media. AJR Am J Roentgenol 171:941–949
17. Yuan F, Salehi HA, Boucher Y et al (1994) Vascular permeability and microcirculation of gliomas and mammary carcinomas transplanted in rat and mouse cranial windows. Cancer Res 54:4564–4568
18. Hashizume H, Baluk P, Morikawa S et al (2000) Openings between defective endothelial cells explain tumor vessel leakiness. Am J Pathol 156:1363–1380
19. Hartmann M, Heiland S, Harting I et al (2003) Distinguishing of primary cerebral lymphoma from high grade glioma with perfusion-weighted magnetic resonance imaging. Neurosci Lett338:119–122
20. Jellinger KA, Paulus W (1992) Primary CNS lymphomas—an update. J Cancer Res Clin Oncol 119:7–27
21. Coulon A, Lafitte F, Hoang-Xuan K et al (2002) Radiographic findings in 37 cases of primary CNS lymphoma in immunocompetent patient. Eur Radiol 12:329–340
22. Roman-Goldstein SM, Goldman DL, Howieson J, Belkin R et al (1992) Primary CNS lymphoma in immunologically normal patients. AJNR Am J Neuroradiol 13:1207–1213

23. Abrey LE, Yahalom J, DeAngelis LM et al (2000) Treatment for primary CNS lymphoma: the next step. J Clin Oncol 18:3144–3150
24. Burger PC, Vogel FS, Green SB et al (1985) Glioblastoma multiform and anaplastic astrocytoma: pathologic criteria and prognostic implications. Cancer 56:1106–1111
25. Burger PC, Scheithauer BW (1994) Tumors of the central nervous system. Armed Forces Institute of Pathology, Washington D.C.
26. Kelly PJ, Daumas-Duport C, Scheithauer BW et al (1987) Stereotactic histologic correlations of computed tomography and magnetic resonance imaging-defined abnormalities in patients with glial neoplasms. Mayo Clin Proc 62:450–459
27. Jackson RJ, Fuller GN, Abi-Said D et al (2001) Limitations of stereotactic biopsy in the initial management of gliomas. Neurooncology 3:193–200
28. Wesseling P, Ruiter DJ, Burger PC (1997) Angiogenesis in brain tumors: pathobiological and clinical aspects. J Neurooncol 32:253–265
29. Tofts PS, Brix G, Buckley DL et al (1999) Estimating kinetic parameters from dynamic contrast-enhanced T(1)-weighted MRI of a diffusable tracer: standardized quantities and symbols. J Magn Reson Imaging 10:223–232